Cumhuriyet Sci. J., 44(4) (2023) 723-732
DOI: https://doi.org/10.17776/csj.1375105

Cumhuriyet Science Journal

| csj.cumhuriyet.edu.tr | Founded: 2002 ISSN: 2587-2680 e-ISSN: 2587-246X Publisher: Sivas Cumhuriyet University

Investigation of Antiviral Activities of Nickel and Copper Complexes with Macrocyclic Ligands against Crimean-Congo Hemorrhagic Fever by In Silico Calculations

Sultan Erkan [1,a,*], Niyazi Bulut [2,b], Duran Karakaş [1,c]

[1] *Chemistry Department, Science Faculty, Sivas Cumhuriyet University, Sivas, Türkiye*
[2] *Department of Physics, Faculty of Science, Fırat University, 23119, Elazığ, Türkiye*
**Corresponding author*

Research Article

History
Received: 16/10/2022
Accepted: 15/12/2023

ABSTRACT

For the first time, electronic characteristics of potential drug candidates and their inhibitory activities have been linked thanks to this work. Synthesized copper and nickel complexes with trans-N1,N8-bis(2-cyanoethyl)-2,4,4,9,11,11-hexamethyl-1,5,8,12-tetraazacyclotetradecane (tet-bx) ligand, as well as the proposed hypothetical complexes, were properly examined by the appropriate calculation method in atomic and molecular dimensions. The appropriate calculation level was achieved by using the IR spectroscopic data of the tet-bx ligand. The experimental and calculated bond stretching frequencies were compared for synthesized complexes $[Ni(tet\text{-}bx)](ClO_4)_2$ (1), $[Cu(tet\text{-}bx)](ClO_4)_2$ (2), $[Ni(tet\text{-}bx)(NCS)_2]$ (3), and $[Ni(tet\text{-}bx)(ClO_4)Cl]$ (5). Some bond stretching frequencies of hypothetical complexes $[Cu(tet\text{-}bx)(NCS)_2]$ (4) and $[Cu(tet\text{-}bx)(ClO_4)Cl]$ (6) have also been proposed and their molecular structure were determined. To analyze the electronic behavior of the examined complexes at the atomic level, Fukui function indices (nucleophilic f^+ and electrophilic f^- populations) were determined. Furthermore, antibacterial and antiviral inhibition efficiency of the complexes against Crimean-Congo hemorrhagic fever has been investigated by docking studies.

Keywords: Fukui function indices, Molecular docking, Crimean-Congo.

[a] *sultanerkan58@gmail.com* *https://orcid.org/0000-0001-6744-929X*
[b] *bulut_niyazi@yahoo.com* *https://orcid.org/0000-0003-2863-7700*
[c] *dkarakas@cumhuriyet.edu.tr* *https://orcid.org/0000-0002-6770-3726*

Introduction

Macrocyclic ligands and their metal complexes have a wide field of study in coordination chemistry. Tetraazamacrocyclic ligands provide application area with wide perspective thanks to donor nitrogen atoms. Metal ions can bind to the macrocyclic cavity [1,2]. In addition, their electronic behaviour may change by the donor and accepting groups. Complexes with macrocyclic ligands are called chelates. Chelates are of biological importance due to activities of antibacterial, antifungal and antitumor. Therefore, chelates have been evaluated in the pharmacological field [3]. In recent years, they have been used as contrast-enhanced magnetic resonance imaging (MRI) agents and even radio immunotherapeutic agents in the field of radiology [4].

In recent years a number of compounds to be tested can be reduced and the design based on the structure required in treatment can be provided thanks to the in silico (or virtual) compound design [5]. The pharmaceutical industry increasingly uses modern medicinal chemistry methods with molecular modelling [6]. Molecular and structural drug design has been developed with spectroscopic methods. In this way, the three-dimensional protein structure is obtained and provided structural information about drug targets and drug candidates [7]. Drug candidate compounds are interacted with target proteins representing biological structures with the aid of simulation [8].

Crimean-Congo haemorrhagic fever (CCHFV) is a tick-borne viral disease. The efficacy of therapeutic options has not been proven in clinical trials for viral disease with a high mortality rate [9]. Drug developments that can be the basis of treatment continue [10].

In this study, synthesized and hypothetical complexes are investigated by computational chemistry methods. The appropriate calculation level is determined according to some bond stretching frequencies of tet-bx ligand. IR spectra of previously synthesized complexes (1), (2), (3) and (5) are computed with the appropriate computational level and are compared with the experimental data. IR spectra of the (4) and (6) hypothetical complexes are proposed. The nucleophilic and electrophilic behaviours of the atoms in the studied complexes can be separated by Fukui function indices. Antibacterial properties are examined and detailed with the help of molecular docking. From the docking results of the investigated complexes, their suitability for Crimean-Congo haemorrhagic fever is discussed. In docking studies, the types of interaction between the amino acid residues of target proteins and the atoms in the complexes are examined. The behaviour of the atoms that play an active role in the interaction types of (1) - (6) complexes are

compared with the electronic behaviours obtained from Fukui functions.

Materials and Methods

The complexes structures of (1) - (6) were drawn in the GaussView 6.0.16 program [11]. Optimization and vibration frequency calculations for tet-bx were made at B3LYP, B3PW91 and M062X methods [12-14]. LANL2DZ (for metal atoms) [15] and 6-31G(d) (for other atoms) [16] basis sets used for electron spin selection. All calculations performed in Gaussian 09: AS64L-G09RevD.01 program and no imaginary frequency was obtained [17]. The complexes and proteins examined in MMFF94 method were optimized with DockingServer [18]. Charge calculations were carried out using the Gasteiger method. Neutral medium (pH = 7.0) was used in all calculations. The dimensions of the grid maps were 90 × 90 × 90 Å (x, y and z) and were calculated by the Solis Wets local search method and Lamarckian genetic algorithm [19].

Result and Discussion

Determination of Calculation Level

One of the spectroscopic analysis methods that may be obtained in depth using computational chemistry approaches is the infrared spectrum. It's also one of the factors that goes into choosing the calculation level [20]. The field of study offers quite a lot of computation levels with many methods and basis sets. Density Functional Theory (DFT) is an approach that gives the most reasonable results. For this purpose, the B3LYP, B3PW91 and M062X methods were chosen for including the DFT. As the basis set, LANL2DZ for metal atoms and 6-31G(d) for other atoms were preferred. The experimental and calculated with different DFT methods some vibrational frequencies and the corresponding regression coefficient (R^2) values are given in Table 1 for the tet-bx ligand and the molecular structure are pictured in Figure 1.

Table 1. Some experimental and calculated stretching frequencies of tet-bx ligand.

	Exp.	B3LYP	B3PW91	M062X
νN-H	3271	3448	3434	3300
νC-H	2965	2946	2928	2973
νCH_3	1385	1431	1416	1367
νC–C	1141	1236	1217	1179
νC≡N	2245	2342	2338	2315
R^2	-	0.9943	0.9941	0.9988

Vibration frequencies are in cm^{-1} unit.

The calculated frequencies listed in Table 1 are the anharmonic frequencies. Anharmonic frequencies are obtained by multiplying the harmonic frequencies with the scale factor suitable for the studying level.

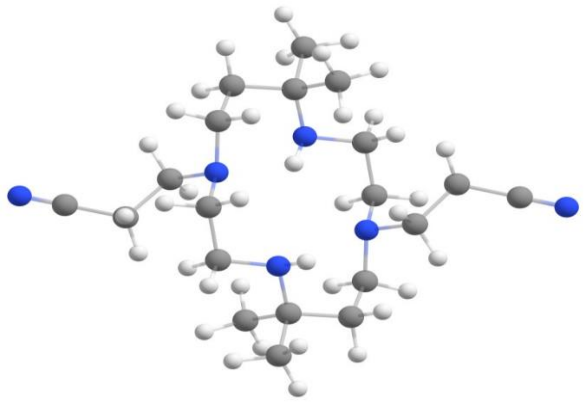

Figure 1. Optimized structure of tet-bx ligand.

The scale factor for B3LYP/6-31g(d) and B3PW91/6-31g(d) levels were taken as 0.991 and 0.986, respectively [21]. The scale factor is selected as 0.9496 for level M062X/6-31G(d) [22]. The N-H bond stretching frequency obtained at the experimental 3271 cm^{-1} was calculated as 3300 cm^{-1} at the M062X/6-31G(d) level. The C-H bond stretching frequency with an experimental value of 2965 cm^{-1} was calculated as 2946 cm^{-1} with B3LYP, 2928 cm^{-1} with B3PW91 and 2973 cm^{-1} with M062X. As seen in Table 1, the closest experimental value for CH_3 bond stretching was obtained as 1367 cm^{-1} at the M062X level. The calculated values of the C≡N bond stretching are 2342 cm^{-1} for B3LYP, 2338 cm^{-1} for B3PW91 and 2315 cm^{-1} for M062X. As a result, the most suitable level was determined as M062X/6-31G(d) level. According to the simple linear regression analysis, the calculation level with R^2 value close to 1 was used for other calculations.

Optimized Structure

[Ni(tet-bx)$(ClO_4)_2$] (1), [Cu(tet-bx)$(ClO_4)_2$] (2), [Ni(tet-bx)$(NCS)_2$] (3) and [Ni(tet-bx)(ClO_4)Cl] (5) complexes were synthesized by Roy et al at 2021 [23]. In addition to nickel complexes, hypothetical copper complexes ([Cu(tet-bx)$(NCS)_2$] (4) and [Cu(tet-bx)Cl(ClO_4)] (6)) were also investigated considering the difference in molecular properties of electron-releasing (ClO_4, NCS) and electron donating (Cl) groups with inductive effect. Figure 2 depicts the optimal structures of the hexamethyl tetraazamacrocyclic ligand, as well as synthetic and hypothesized nickel-copper complexes containing this ligand. These structures were discovered at M062X/LANL2DZ/6-31G(d) in the gas phase.

The molecular properties of these electron-rich structures, which are quite large in volume and difficult to analyze, are quite a struggle at the molecular level. It has been observed that the optimized structures form the six coordinated octahedral nickel (II) and copper (II) complexes by axial addition of the four coordinated square-planar nickel (II) and copper (II) complexes.

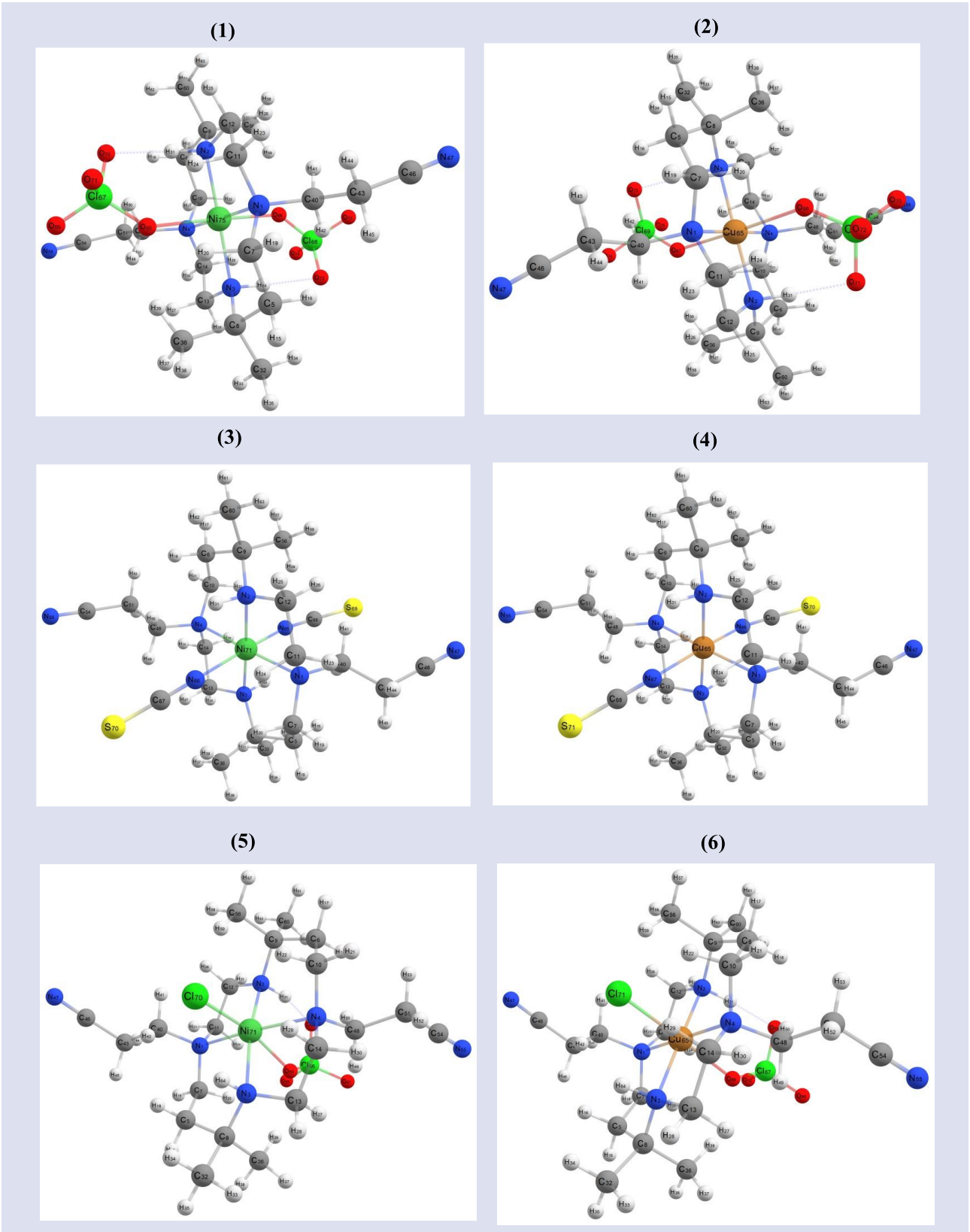

Figure 2. Optimized structure of investigated complexes.

IR Spectra Analysis

IR spectra of the studied complexes were calculated to obtain information about functional groups. For this purpose, IR spectra of the synthesized complexes ((1), (2), (3) and (5)) and hypothetical complexes ((4) and (6)) are listed in Table 2. The results of the spectrums calculated at the M062X/LANL2DZ/6-31G(d) level were compared with the experimental data. In this analysis, the peaks with the highest intensity were taken into account. In this analysis, labeling was made with the help of the animation, considering the peaks with the highest intensity.

Table 2. IR spectral data of the metal complexes.

Comp.	(1)		(2)		(3)		(4)	(5)		(6)
Modes	**Exp.**	**Calc.**	**Exp.**	**Calc.**	**Exp.**	**Calc.**	**Calc.**	**Exp.**	**Calc.**	**Calc.**
νN-H	3167	3207	3182	3190	3217	3270	3376	3147	3223	3214
νC-H	2997	3004	2974	2953	2970	2955	2928	2960	2954	2924
νCH3	1383	1372	1380	1359	1381	1373	1413	1371	1358	1354
νC–C	1157	1151	1153	1148	1180	1171	1119	1186	1181	1172
νM-N	532		538	536	540	545	566	522	522	515
νC≡N	2245	2319	2256	2313	2249	2301	2319	2245	2316	2311
νCl-O	1087	1053	1087	1084	-	-	-	1095	1068	1066
νM-N	624	596	-	-	-	-	-	613	577	-
νM-Cl	-	-	-	-	-	-	-	-	-	873
νM-O	-	-	1041	976	-	-	-	-	-	-
νC≡N	-	-	-	-	2063	2063	-	-	-	-
νCN							1030	-	-	-
νCS	-	-	-	-	862	773	800	-	-	-
δNCS	-	-	-	-	478	474	-	-	-	-

ν: stretching, δ: Scissoring

When looking at the data in Table 2, it was discovered that the analyzed complexes peaked at similar frequencies. The designation of frequencies that qualify empirically as other is a specific distinction in this section. Complex (1) has an experimental value of 1087 cm^{-1}, which corresponds to a calculated Cl-O bond stretching frequency of 1053 cm^{-1}. In addition, the experimental frequency at 624 cm^{-1} was labeled as the metal nitrogen vibration mode at 596 cm^{-1}. Experimental Cl-O bond stretching frequency for complex (2), at 1087 cm^{-1} was calculated as 1084 cm^{-1}, and M-O bond stretching frequency at 1041 cm^{-1} was computed as 976 cm^{-1}. The calculated results are quite compatible with the experimental values according to the relevant labeling. In addition, the scissoring mode was experimentally found to be 478 cm^{-1}. In the calculation, it was determined as scissoring mode at 474 cm^{-1}. Scissoring mode for complex (3), has been taken into account as it is a high-intensity peak. Depending on the harmony of the experimental and the calculation results, the bond stretching frequencies of the hypothetical complexes (4) and (6) can be boldly suggested. The bond stretching frequency for complex (4) at 1030 cm^{-1} was assigned to bond stretching containing the single bond carbon-nitrogen. The frequency at 800 cm^{-1} is the C-S bond stretching mode. For complex (6), the frequency at 1066 cm^{-1} was labeled as Cl-O bond stretching with the help of animation.

Chemical Reactivity

Computational chemistry methods allow reactivity analysis of the chemical species under study. The reactivity analysis of a chemical species can be interpreted by the quantum chemical parameters such as hardness (η), softness (σ), chemical potential (μ) and electronegativity (χ). Relevant parameters for reactivity analysis of ligands and complexes were calculated with Equations (1)-(3) and given in Table 3.

$$\mu = -\chi = \left[\frac{\partial E}{\partial N}\right]_{\nu(r)} = -\left(\frac{I+A}{2}\right) \quad (1)$$

$$\eta = \frac{1}{2}\left[\frac{\partial^2 E}{\partial N^2}\right]_{\nu(r)} = \frac{I-A}{2} \quad (2)$$

$$\sigma = 1/\eta \quad (3)$$

Table 3. Quantum chemical parameters of metal complexes.

Compounds	η (eV)	σ (eV^{-1})	X (eV)	μ (eV^{-1})
(1)	3.4247	0.2920	4.4656	-4.4656
(2)	5.0838	0.1967	3.8465	-3.8465
(3)	2.8458	0.3514	3.9879	-3.9879
(4)	3.6542	0.2737	2.4558	-2.4558
(5)	3.4247	0.2920	4.4656	-4.4656
(6)	4.7216	0.2118	3.6593	-3.6593

When Table 3 is examined for the reactivity relationship of the complexes, it is noted that the hardness parameter of copper complexes is generally higher. In relation to this parameter, the softness value of complex (3) is the highest. Hard molecules have high energy gap values and softness is the multiplicative inverse of hardness. According to the Maximum Hardness Principle, molecules arrange themselves to be as hard as possible. Therefore, chemical hardness is a measure of stability.

Electronic Behavior of Atoms in the Complexes

The major aim of this part is to investigate the molecular behavioural aspects of atomic locations in pharmacological investigations. In drug design, predicting of the charge of the atoms in complex it can be useful. In this study, Fukui function indices are used to predict the electronic behaviour of atoms in studied complexes. The electronic density of the system against the number of electrons at a constant external potential is used to calculate Fukui functions using the finite difference

approximation of the first derivative. Fukui functions, according to this method, are provided by the following Equations (4)- (6) [24].

$$f_k^+ = q_k(N+1) - q_k(N) \quad (4)$$

$$f_k^- = q_k(N) - q_k(N-1) \quad (5)$$

$$f_k^0 = \frac{1}{2}\left[q_k(N+1) - q_k(N-1)\right] \quad (6)$$

From top to bottom, these equations reflect the selectivity of a molecule's nucleophilic, electrophilic, and radical attack sites, respectively. In neutral (N), anionic (N+1), and cationic (N-1) states, q_k is the atomic charges in the kth atomic region of a molecule. Fukui function indices of the investigated complexes are given Table S1-S3 and Figure S1. The Fukui function indices of the atoms in the complexes are given graphically in Figure 3, except for indices in the range 0-0.01. The f^+ and f^- values are considered while describing donor-receptor interactions. Electronically, the nucleophilic (f^+) and electrophilic (f^-) populations correspond to Fukui function indices of atomic sites. Positive values are denoted by (f^+), whereas negative values are denoted by (f^-). The tendency to donate electrons increases with increasing positive charge.

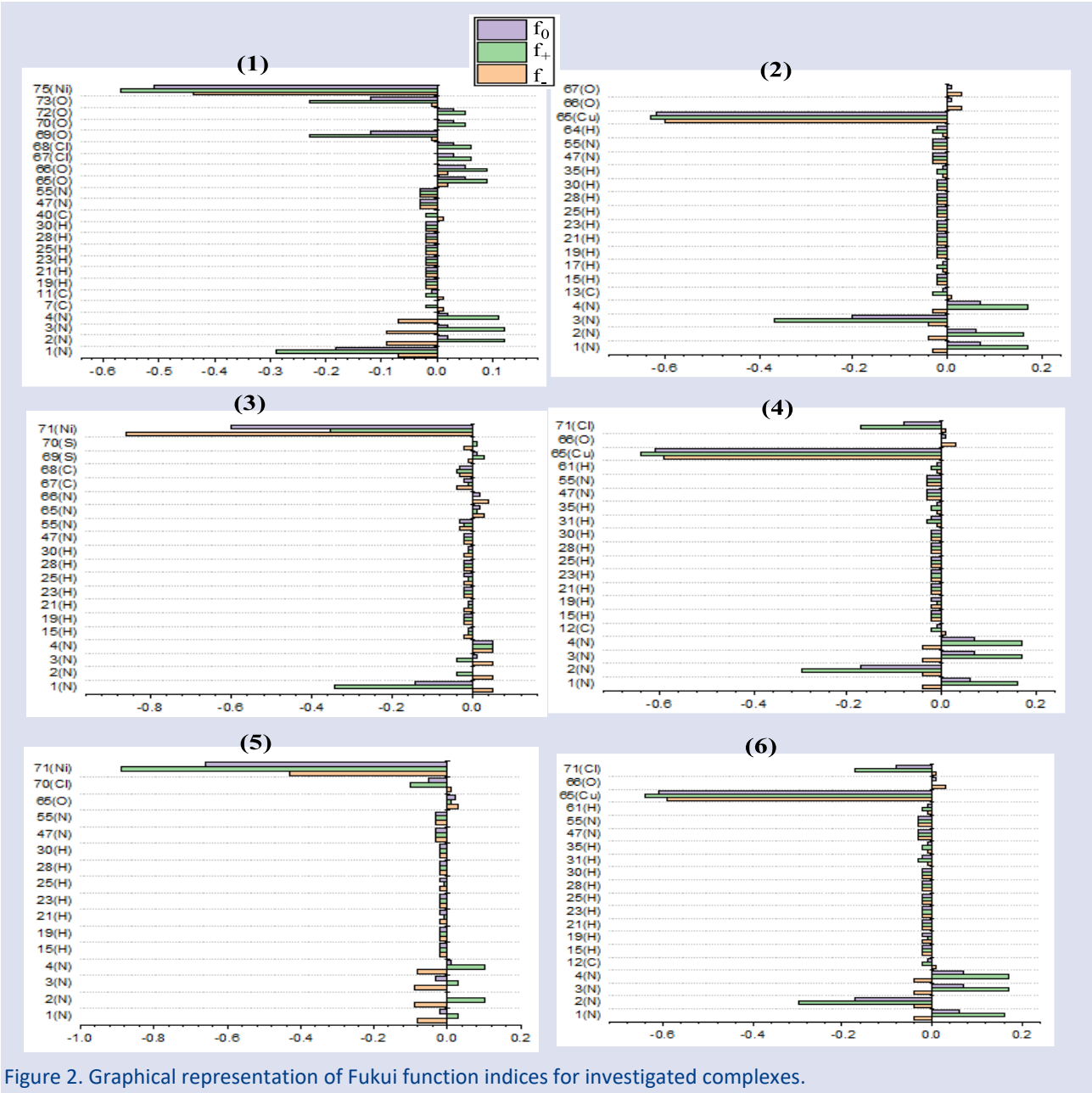

Figure 2. Graphical representation of Fukui function indices for investigated complexes.

With increasing negative charge, the ability of atomic sites to receive electrons increases. Metal atoms in all complexes have the biggest negative peak in terms of Fukui function indices, as seen in Figure 3. The electrical behaviour, on the other hand, varies depending on the type of metal and the ligand connected to it. The electrical richness of metal complexes is analogous to this condition.

The electrophilic property of the metal atoms in the complexes appears to be more prominent. Furthermore, 73O, 69O and 1N electrophilic, 2N, 3N, 4N, and other

oxygen atoms exhibit nucleophilic activity in complex (1). The 1N and 2N act as electron donors in complex (2), whereas the 3N and 4N act as electron acceptors. Complexes (3) with 70S and 1N atoms and complex (4) with 71Cl and 2N atoms have a high potential to receive electrons. In complex (5), 1N and 3N atoms have a strong inclination to gain electrons, whereas the 1N, 3N and 4N atoms in complex (6) have a strong inclination to donate electrons.

Molecular Docking Studies

Molecular docking studies allow to examine drug design at the molecular atomic level. Binding energies and interaction types of the drug candidate substances with the proteins can be determined with molecular docking studies. Thus, it can be predicted whether the drug candidate molecule has anticancer, antibacterial, antifungal and antiviral properties. Cellular sized protein structures are obtained from the protein data bank. Amino acid residues in each protein with drug candidate molecules exhibit different types of interaction. It has been stated that the previously synthesized complexes (1), (2), (3) and (5) have antimicrobial activity against Bacillus cereus, Staphylococcus aureus, Salmonella typhi and Pseudomonus aeruginosa. Protein codes for these gram-positive bacteria species and gram-negative bacteria species are 5V8E [25], 5YHG [26], 6V4O [27] and 4NX9 [28], respectively.

In addition to docking studies against bacterial cell types, there is still an undeveloped pharmaceutical industry for Crimean Congo haemorrhagic fever. The inhibition efficiency of the complexes examined with the help of docking will be investigated for this viral disease, which has caused the increase in mortality rates in recent years. There are five different protein structures of the Crimean-Congo haemorrhagic disease determined in the literature. These are Crimean Congo Haemorrhagic Fever Gn zinc finger (PDB ID=2L7X) [29], Structural analysis of a viral OTU domain protease from the Crimean-Congo Haemorrhagic Fever virus in complex with human ubiquitin (PDB ID=3PRP) [30], Envelope glycoprotein from tick-borne encephalitis virus (PDB ID=1SVB) [31], A RNA binding protein from Crimean-Congo haemorrhagic fever virus (PDB ID=3U3I) [32] and The cryo-EM structure of Tick-borne encephalitis virus complexed with Fab fragment of neutralizing antibody (PDB ID=5O6V) [33]. The binding energies and interaction types of synthesized and hypothetical complexes with target proteins determined for antibacterial and antiviral effects were examined. The effective roles of nucleophilic and electrophilic atoms determined by Fukui function indices were investigated.

To test its antibacterial activity, the studied complexes were docked against 5V8E, 5YHG, 6V40 and 4NX9 cell lines, and the molecular docking results are given in Table 3. To estimate the antiviral activity, the studied complexes were docked against the 2L7X, 3PRP, 1SVB, 3U3I and 5O6V cell lines and the results are presented in Table 4. Additionally, the secondary chemical interactions between the amino acid residues of the atoms in the complexes are given in Tables 4 and 5 in terms of antibacterial and antiviral, respectively. Moreover, binding modes of studied complexes with the identified 1SVB target proteins are given in Figures 3. For the reliability of the results, calculations were made with and DockingServer [34].

Table 4. Docking energy results of complexes (1)-(6) for antibacterial effect

Complex	5V8E		5YHG		6V40		4NX9	
	E_{Bind}	E_S	E_{Bind}	E_S	E_{Bind}	E_S	E_{Bind}	E_S
(1)	-5.06	-5.36	-9.64	-9.63	-5.56	-5.97	-5.40	-5.26
(2)	-5.97	-6.95	-9.47	-9.78	-5.09	-4.58	-5.16	-4.87
(3)	-6.15	-5.94	-9.49	-9.56	-5.53	-5.30	-5.07	-4.87
(4)	-6.34	-6.97	-8.30	-8.82	-5.84	-4.88	-4.99	-4.59
(5)	-6.13	-7.61	-8.76	-9.05	-4.90	-5.89	-4.97	-4.72
(6)	-5.94	-7.86	-7.79	-8.20	-5.26	-4.52	-4.98	-4.90
Ampicillin	-4.72	-4.57	-4.65	-4.17	-4.04	-4.43	-4.50	-4.45

E_{Bind}: Est. Free Energy of Binding (kcal/mol), E_S: vdW + Hbond + desolve Energy (kcal/mol)

With docking studies in the first step, the antibacterial effects of the complexes on gram-positive and gram-negative bacterial species were investigated. The obtained calculation results and experimental data were compared. According to the experimental data, the inhibition efficiency of complex (3) against Bacillus cereus bacteria species is higher than complexes (1), (2) and (5) [23]. Docking results are consistent with the experimental findings. Because the estimated free energy of binding (E_{Bind}) of complex (3) was calculated as -6.15 kcal/mol in the interaction of the investigated complexes with the 5V8E target protein. This value is greater than the estimated free energy of binding of other complexes and reference material. In addition, it was concluded that the complexes (2), (3) and (5) with the same antibacterial effects had different E_{bind} and Es values according to the docking results.

Table 5. Docking energy results of complexes (1)-(6) for Crimean Congo

Complex	2L7X		3PRP		1SVB		3U3I		5O6V	
	E_{Bind}	E_S	E_{Bind}	E_S	E_{Bind}	E_S	E_{Bind}	E_S	E_{Bind}	E_S
(1)	-4.68	-5.51	+317.06	+312.09	-4.19	-5.44	-4.67	-6.85	-4.01	-4.56
(2)	-5.42	-6.04	+146.59	+139.50	-5.23	-5.59	-5.14	-6.73	-6.03	-6.32
(3)	-5.32	-6.46	+368.02	+365.92	-4.68	-5.17	-5.02	-6.59	-5.79	-6.16
(4)	-5.31	-6.22	+208.49	+206.91	-4.46	-5.21	-5.19	-6.60	-4.80	-5.48
(5)	-5.00	-6.39	+14.74	+12.65	-4.23	-5.66	-4.95	-6.32	-5.23	-6.71
(6)	-5.48	-4.28	+6.40	+3.74	-4.48	-4.75	-5.27	-7.76	-5.35	-5.93
Ribiravin	-4.48	-4.08	-3.65	-4.07	-3.27	-4.39	-3.90	-5.08	-3.22	-3.76

E_{Bind}: Est. Free Energy of Binding (kcal/mol), E_S: vdW + Hbond + desolve Energy (kcal/mol)

The fact that the docking results are highly consistent with the experimental data allows discussing the advantages and disadvantages of all the complexes studied for Crimean-Congo hemorrhagic fever. There are five different protein structures described in the literature for Crimean-Congo hemorrhagic fever. As shown in Table 5, except for 3PRP target protein, Complexes (1) - (6) exhibit higher inhibitory activity than reference Ribiravine. Positive data at E_{Bind} values given in Table 5 indicate that the drug candidate complexes have no inhibitory activity on the related target protein. Negative increase in E_{Bind} values highlights the high inhibitory efficiency of the drug candidate. According to the results from Table 5, in general ClO_4^- substituted copper complexes are more biologically active than ClO_4^- substituted nickel complexes. In addition, the inhibition efficiency of nickel complexes with NCS ligands on target proteins is generally higher than copper complexes with NCS ligands.

The secondary chemical interactions between the investigated complexes and the target proteins were investigated. The types of interaction of complexes (1) - (6) with amino acid residues of antibacterial cell proteins are given in Tables S4-S7 in Supplementary Materials. Data including secondary chemical interactions of complexes with amino acid residues of the target proteins of PDB ID: 2L7X, 3PRP, 3U3I and 5O6V representing Crimean-Congo hemorrhagic fever are given in Tables S8-S12 in the Supplementary Materials. In addition, the interaction types between PDB ID: 1SVG with (1) - (6) are given in Table 6.

Table 6. Interaction types between investigated complexes and 1SVB target protein

	Hydrogen Bonds	Polar	Hydrophobic
(1)- 1SVB	N-LYS284	N-ASN8	C-LEU27
	N-GLY28	N-GLU26	
		N-LYS284	
(2)- 1SVB	N-ASP46	N-ARG2	C-LEU27
		N-TRP44	C-ALA47
		N-LYS284	C-HIS282
(3)- 1SVB	N-LEU27	N-LYS284	C-LEU27
			C-PRO272
			C-VAL273
(4)- 1SVB	N-LEU27	-	C-LEU27
			C-PRO272
			C-VAL273
(5)- 1SVB	N-ASP46	N-ARG2	C-LEU27
		N-TRP44	C-HIS282
		N-ASP46	
		N-ARG160	
		N-LYS284	
(6)- 1SVB	N-VAL273	N-LYS284	C-LEU27
	N-LYS284		C-VAL273

According to Table 6, nitrogen atoms of complex (1) formed H-bond with LYS284 and GLY28 amino acid residues of 1SVB protein. Again, the nitrogen atoms of complex (1) are in polar interaction with the ASN8 amino acid residue of the 1SVB protein. In addition, the carbon atom of complex (1) exhibits hydrophobic interaction with LEU27. The interactions of the other complexes with the amino acid residues of the 1SVB target protein are shown in Table 6. In addition, the mode of binding of the investigated complexes with the 1SVB target protein is given in Figure 4.

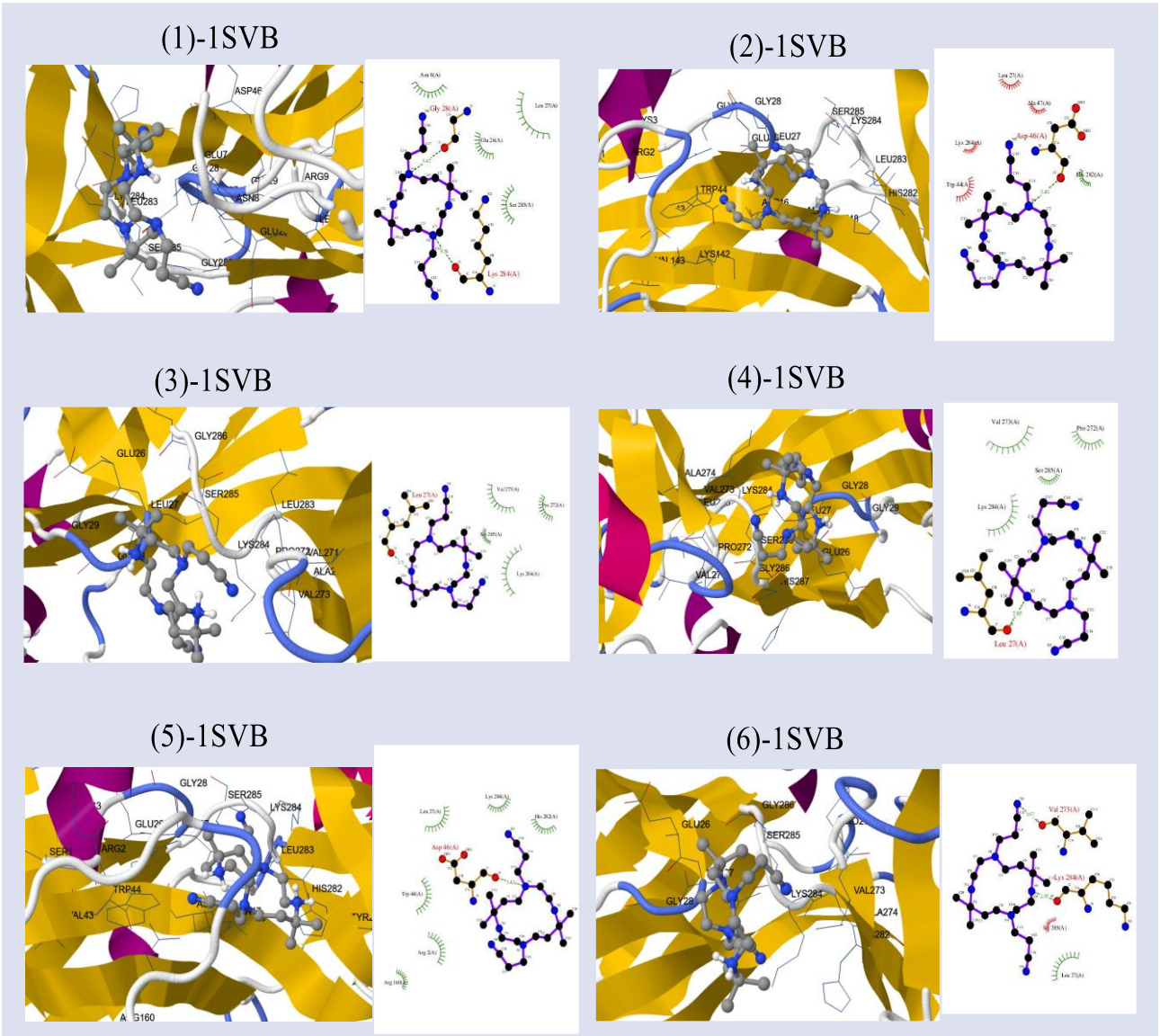

Figure 3. Interaction modes between (1)-(6) complexes and 1SVB target protein.

The investigated interaction results show that the nucleophilic nitrogen atoms obtained from the Fukui functions formed H-bonds with the amino acid residues of the target proteins. Electrophilic nitrogen and carbon atoms determined by Fukui functions exhibit polar interaction and hydrophobic interactions. With this manuscript, which was conducted for the first time in the literature, pioneering approaches for drug development can be presented. Interactions of nucleophilic and electrophilic atoms in drug candidate molecules with target proteins can be predicted in in silico studies. In this way, the interactions of the drug studied in drug modelling with target proteins can be improved and their biological activities can be improved.

Conclusion

The vibrational frequencies of the synthesized tet-bx ligand were compared experimentally and using several DFT approaches. The M062X/6-31g(d) level was judged to be the ideal calculation level based on linear regression coefficients (R^2), and all computational studies were conducted using the M062X approach. Hypothetical complexes (4) and (6) were hypothesized based on the experimentally synthesized complexes (1), (2), (3), and (5). The values calculated with the experimental certain bond stretching frequencies were compared for the complexes (1), (2), (3), and (5), and the experimental and computational data were determined to be comparable according to the comparison results. For the structural investigation of complexes (4) and (6), some needed bond stretching frequencies were provided. Fukui function indices were used to differentiate the nucleophilic and electrophilic characteristics of the atoms in the studied complexes. The biological activities at the molecular level of the complexes whose antibacterial properties were shown to be experimentally high were investigated using docking studies. The complexes' usefulness for the treatment of Crimean-Congo hemorrhagic illness was also studied. The inhibition activities of the complexes on all target proteins in the literature representing the Crimean Congo were investigated. The investigated complexes

yielded higher binding energies compared to the reference Ribiravine with all target proteins except PDB ID: 3PRP. The nucleophilic atoms produced by Fukui functions have been found to have secondary chemical interactions with the target proteins' amino acid residues. Finally, it was determined that the chemical species chosen for drug design against antibacterial and Crimean Congo should have nucleophilic substituent.

Acknowledgments

The numerical calculations reported in this paper were fully/partially performed at TUBITAK ULAKBIM, High Performance and Grid Computing Center (TRUBA resources). NB would like to thank FIRAT University Scientific Research Projects Unit (Project number: FF.20.22).

Conflicts of interest

The authors have made the following contributions to this article. Niyazi Bulut: The calculation of tet-bx ligand and their nickel and copper complexes. Duran Karakaş: Determination of target proteins suitable for antibacterial and Crimean-Congo hemorrhagic fever, creating figures and tables. Sultan Erkan: Design of complexes, the collection and interpretation of all calculation results and writing of the article.

References

[1] Martell, A. E., Smith, R. M., Critical stability constants, vol 3 Plenum Press. New York, NY, (1977).

[2] Hassan, M. M., Kinetics and mechanism of complex formation of a pendant arm macrocycle reacting with copper (II) and mercury (II), *J. Saudi Chem. Soc*., 13(2) (2009) 185-190.

[3] Shankarwar, S. G., Nagolkar, B. B., Shelke, V. A., Chondhekar, T. K., Synthesis, spectral, thermal and antimicrobial studies of transition metal complexes of 14-membered tetraaza [N4] macrocyclic ligand, *Spectrochim. Acta, Part A*, 145 (2015) 188-193.

[4] Bernhardt, P. V., Sharpe, P. C., C-substituted macrocycles as candidates for radioimmunotherapy, Inorg. Chem, 39 (18) (2000) 4123-4129.

[5] Hughes, J. P., Rees, S., Kalindjian, S. B., Philpott, K. L., Principles of early drug discovery, *Br. J. Pharmacol*., 162 (6) (2011) 1239-1249.

[6] Lipinski, C. A., Lombardo, F., Dominy, B. W., Feeney, P. J., Experimental and computational approaches to estimate solubility and permeability in drug discovery and development settings, *Adv. Drug Delivery Rev*., 23(1-3) (1997) 3-25.

[7] Erkan, S., Activity of the rocuronium molecule and its derivatives: A theoretical calculation, *J. Mol. Struct*., 1189 (2019) 257-264.

[8] Kaya, S., Erkan, S., Karakaş, D., Computational investigation of molecular structures, spectroscopic properties and antitumor-antibacterial activities of some Schiff bases, Spectrochim, *Acta, Part A*, 244 (2021) 118829.

[9] Zivcec, M., Scholte, F. E., Spiropoulou, C. F., Spengler, J. R., Bergeron, É., Molecular insights into Crimean-Congo hemorrhagic fever virus, Viruses, 8(4) (2016) 106.

[10] Guo, Y., Wang, W., Ji, W., Deng, M., Sun, Y., Zhou, H., ... Rao, Z., Crimean–Congo hemorrhagic fever virus nucleoprotein reveals endonuclease activity in bunyaviruses, *Proc. Natl. Acad. Sci. U.S.A*., 109(13) (2012) 5046-5051.

[11] Sharifi, A., Amanlou, A., Moosavi-Movahedi, F., Golestanian, S., Amanlou, M., Tetracyclines as a potential antiviral therapy against Crimean Congo hemorrhagic fever virus: Docking and molecular dynamic studies, *Comput. Biol. Chem*., 70 (2017) 1-6.

[12] R.D. Dennington, T.A. Keith, J.M. Millam, GaussView 6.0. 16, Semichem. Inc., Shawnee Mission KS, 2016.

[13] Becke, A. D. Perspective: Fifty years of density-functional theory in chemical physics, *J. Chem. Phys*., 140(18) (2014) 18A301.

[14] Lee, C., Yang, W., Parr, R. G., Development of the Colle-Salvetti correlation-energy formula into a functional of the electron density, *Phys. Rev. B*, 37(2) (1988) 785.

[15] Zhao, Y., Truhlar, D. G., The M06 suite of density functionals for main group thermochemistry, thermochemical kinetics, noncovalent interactions, excited states, and transition elements: two new functionals and systematic testing of four M06-class functionals and 12 other functionals, *Theor. Chem. Acc*., 120(1-3) (2008) 215-241.

[16] Check, C. E., Faust, T. O., Bailey, J. M., Wright, B. J., Gilbert, T. M., Sunderlin, L. S., Addition of polarization and diffuse functions to the LANL2DZ basis set for p-block elements, *J. Phys. Chem. A*, 105(34) (2001) 8111-8116.

[17] Rassolov, V.A., Ratner, M.A., Pople, J.A., Redfern, P.C., Curtiss, L.A., 6-31G* basis set for third-row atoms, *J. Comput. Chem*., 22 (9) (2001) 976–984.

[18] Frisch, M.J., Trucks, G.W., Schlegel, H.B., Scuseria, G.E., Robb, M.A., Cheeseman,J.R., ... Nakatsuji, H., Gaussian09 Revision D. 01, Gaussian Inc.,Wallingford CT, 2009. http://www.gaussian.com.

[19] Bikadi, Z., Hazai, E., Application of the PM6 semi-empirical method to modeling proteins enhances docking accuracy of AutoDock, J. Cheminform, 1(1) (2009) 1-16. https://www.dockingserver.com/web

[20] Güzel, E., Koçyiğit, Ü. M., Taslimi, P., Erkan, S., Taskin, O. S., Biologically active phthalocyanine metal complexes: Preparation, evaluation of α-glycosidase and anticholinesterase enzyme inhibition activities, and molecular docking studies, *J. Biochem. Mol. Toxicol*., (2021) e22765.

[21] Zapata Trujillo, Juan C.; Mckemmish, Laura K. Meta-analysis of uniform scaling factors for harmonic frequency calculations, Wiley Interdiscip. Rev., *Comput. Mol. Sci.,* 12 (2022) 1584.

[22] Ünal, Y., Nassif, W., Özaydin, B. C., Sayin, K. Scale factor database for the vibration frequencies calculated in M06-2X, one of the DFT methods, *Vib. Spectrosc*., 112 (2021) 103189.

[23] Dey, L., Rabi, S., Hazari, S. K. S., Roy, T. G., Buchholz, A., Plass, W. Copper (II) and nickel (II) complexes of an N-pendent bis-(cyanoethyl) derivative of an isomeric hexamethyl tetraazamarocyclic ligand: Synthesis, characterization, electrolytic behavior and antimicrobial studies, *Inorg. Chim. Acta*, 517 (2021) 120172.

[24] R.B. Woodward and R. Hoffmann, *J. Amer. Chem. Soc*., 87 395 (1965)

[25] Sychantha, D., Little, D. J., Chapman, R. N., Boons, G. J., Robinson, H., Howell, P. L., Clarke, A. J. PatB1 is an O-acetyltransferase that decorates secondary cell wall polysaccharides, *Nat. Chem. Biol.*, 14(1) (2018) 79.

[26] Song, L., Zhang, Y., Chen, W., Gu, T., Zhang, S. Y., Ji, Q., Mechanistic insights into staphylopine-mediated metal acquisition, *Proc. Natl. Acad. Sci. U.S.A.,* 115(15) (2018) 3942-3947.

[27] Madsen, A., Dai, Y. N., McMahon, M., Schmitz, A. J., Turner, J. S., Tan, J., ... Ellebedy, A. H., Human antibodies targeting influenza B virus neuraminidase active site are broadly protective, *Immunity*, 53(4) (2020) 852-863.

[28] Song, W. S., Yoon, S. I., Crystal structure of FliC flagellin from Pseudomonas aeruginosa and its implication in TLR5 binding and formation of the flagellar filament, *Biochem. Biophys. Res. Commun.*, 444(2) (2014) 109-115.

[29] Estrada, D. F., De Guzman, R. N., Structural characterization of the Crimean-Congo hemorrhagic fever virus Gn tail provides insight into virus assembly, *J. Biol. Chem.*, 286(24) (2011) 21678-21686.

[30] Capodagli, G. C., McKercher, M. A., Baker, E. A., Masters, E. M., Brunzelle, J. S., Pegan, S. D., Structural analysis of a viral ovarian tumor domain protease from the Crimean-Congo hemorrhagic fever virus in complex with covalently bonded ubiquitin, *J. Virol.,* 85(7) (2011) 3621-3630.

[31] Rey, F. A., Heinz, F. X., Mandl, C., Kunz, C., Harrison, S. C., The envelope glycoprotein from tick-borne encephalitis virus at 2 Å resolution, *Nature*, 375(6529) (1995) 291-298.

[32] Guo, Y., Wang, W., Ji, W., Deng, M., Sun, Y., Zhou, H., ... Rao, Z., Crimean–Congo hemorrhagic fever virus nucleoprotein reveals endonuclease activity in bunyaviruses, *Proc. Natl. Acad. Sci. U.S.A.,* 109(13) (2012) 5046-5051.

[33] Füzik, T., Formanová, P., Růžek, D., Yoshii, K., Niedrig, M., Plevka, P., Structure of tick-borne encephalitis virus and its neutralization by a monoclonal antibody, *Nat. Commun*., 9(1) (2018) 1-11.

[34] Huey, R., Morris, G. M., Olson, A. J., Goodsell, D. S., A semiempirical free energy force field with charge-based desolvation, *J. Comput. Chem*., 28(6) (2007) 1145-1152.